SUPPORTING INFORMATION

Structural and Luminescence Properties of Heteronuclear Gold(I)/Thallium(I) Complexes Featuring Metallophilic interactions Tuned by Quinoline Pendant Arm Derivatives of Mixed Donor Macrocycles

Rocío Donamaría,[†] Vito Lippolis,[*, ‡] José M. López-de-Luzuriaga,[*, †] Miguel Monge,[†] Mattia Nieddu,[†, ‡] M. Elena Olmos[*,†]

[†] Departamento de Química. Universidad de la Rioja. Centro de Investigación en Síntesis Química (CISQ). Complejo Científico Tecnológico 26004-Logroño, SPAIN.

[‡] Dipartimento di Scienze Chimiche e Geologiche, Università degli Studi di Cagliari, S. S. 554 bivio per Sestu, 09042 Monserrato (Cagliari), Italy.

Table S1. Selected bond lengths [Å] and angles [°] for compound **1·½**toluene.

Tl(1)-Au(1)	3.0597(4)
Au(1)-C(1)	2.043(7)
Au(1)-C(7)	2.034(7)
Tl(1)-S(2)	3.1358(17)
Tl(1)-N(1)	2.913(6)
Tl(1)-N(2)	2.902(5)
Tl(1)-N(3)	2.963(5)
Tl(1)-N(4)	2.944(7)
Tl(1)-F(10)	3.329(4)

Au(1)-Tl(1)-S(2)	71.08(3)
C(7)-Au(1)-C(1)	175.6(3)
C(7)-Au(1)-Tl(1)	95.19(18)
C(1)-Au(1)-Tl(1)	88.99(18)

Table S2. Selected bond lengths [Å] and angles [°] for compound **2**.

Au(1)-Tl(1)	3.2339(4)
Au(1)-C(1)	2.046(7)
Au(1)-C(7)	2.042(7)
Tl(1)-S(1)	3.183(3)
Tl(1)-S(2)	3.128(2)
Tl(1)-N(1)	2.778(6)
Tl(1)-N(2)	2.664(7)
Tl(1)-O(1)	3.034(6)
Tl(1)-F(1)	3.263(5)

C(7)-Au(1)-C(1)	177.2(3)
C(7)-Au(1)-Tl(1)	91.5(2)
C(1)-Au(1)-Tl(1)	86.8(2)
N(2)-Tl(1)-N(1)	62.7(2)
N(2)-Tl(1)-S(2)	81.25(14)
N(1)-Tl(1)-S(2)	69.42(14)
N(2)-Tl(1)-Au(1)	97.52(14)
N(1)-Tl(1)-Au(1)	129.79(13)
S(2)-Tl(1)-Au(1)	157.72(4)

Table S3. Selected bond lengths [Å] and angles [°] for compound **3**·¼CH_2Cl_2.[a]

Au(1)-Tl(1)	3.1999(8)
Au(1)-Tl(2)#1	3.4513(7)
Au(2)-Tl(2)	3.0422(6)
Tl(1)-Tl(2)	3.8865(7)
Au(1)-C(1)	2.087(7)
Au(1)-C(7)	2.093(9)
Au(2)-C(19)	2.034(11)
Au(2)-C(13)	2.054(12)
Tl(1)-N(1)	2.677(10)
Tl(1)-N(2)	2.694(10)
Tl(1)-S(1)	3.283(3)
Tl(1)-S(2)	3.254(4)
Tl(1)-F(1)#1	2.978(9)
Tl(1)-F(10)#1	3.335(16)
Tl(2)-N(3)	2.816(9)
Tl(2)-N(4)	2.695(9)
Tl(2)-S(1)	3.460(4)
Tl(2)-S(2)	3.516(3)

C(1)-Au(1)-C(7)	173.1(4)
Tl(1)-Au(1)-Tl(2)#1	126.90(2)
C(1)-Au(1)-Tl(1)	80.4(3)
C(7)-Au(1)-Tl(1)	102.3(3)
C(1)-Au(1)-Tl(2)#1	92.5(3)
C(7)-Au(1)-Tl(2)#1	90.8(3)
C(19)-Au(2)-C(13)	175.4(4)
C(19)-Au(2)-Tl(2)	96.6(3)
C(13)-Au(2)-Tl(2)	87.6(3)
N(1)-Tl(1)-N(2)	61.3(3)
N(1)-Tl(1)-Au(1)	87.0(2)
N(2)-Tl(1)-Au(1)	79.3(2)
N(4)-Tl(2)-N(3)	63.5(3)
N(4)-Tl(2)-Au(2)	85.56(19)
N(3)-Tl(2)-Au(2)	90.52(17)
N(4)-Tl(2)-Au(1)#1	128.4(2)
N(3)-Tl(2)-Au(1)#1	149.64(18)
Au(2)-Tl(2)-Au(1)#1	116.449(19)

[a] Symmetry transformations used to generate equivalent atoms: #1 = -x, -y+2, -z+1.

Table S4. Selected bond lengths [Å] and angles [°] for **4**·¼CH_2Cl_2.[a]

Tl(1)-Au(1)	3.0852(8)
Tl(1)-Au(2)	3.0216(8)
Tl(1)-Au(1)#1	3.0807(8)
Au(1)-Tl(1)#2	3.0808(8)
Tl(2)-Au(2)	3.3124(8)
Tl(3)-Au(3)	3.0488(8)
Tl(3)-Au(4)	3.0712(8)
Tl(3)-Au(4)#3	3.0500(7)
Au(4)-Tl(3)#4	3.0500(7)
Tl(4)-Au(3)	3.4806(8)
Tl(1)-F(11)	2.923(9)
Tl(1)-F(20)	2.806(11)
Tl(1)-F(5)#1	3.412(10)
Tl(1)-F(6)#1	3.096(10)
Tl(1)-S(4)	3.434(4)
Tl(2)-N(3)	2.684(12)
Tl(2)-N(4)	2.732(10)
Tl(2)-S(3)	3.194(4)
Tl(2)-S(4)	3.152(3)
Tl(2)-O(2)	3.014(11)
Tl(3)-S(1)	3.256(4)
Tl(3)-F(21)	3.017(9)
Tl(3)-F(30)	3.024(11)
Tl(3)-F(31)	3.188(10)
Tl(3)-F(40)	3.123(9)
Tl(4)-N(1)	2.691(12)
Tl(4)-N(2)	2.780(12)
Tl(4)-S(1)	3.182(3)
Tl(4)-S(2)	3.235(4)
Tl(4)-O(1)	3.227(11)
Au(1)-C(1)	2.021(14)
Au(1)-C(7)	2.033(14)
Au(2)-C(13)	2.037(15)
Au(2)-C(19)	2.045(16)
Au(3)-C(25)	2.060(14)
Au(3)-C(31)	2.071(14)
Au(4)-C(43)	2.068(14)
Au(4)-C(37)	2.070(14)

Au(2)-Tl(1)-Au(1)#1	68.593(18)
Au(2)-Tl(1)-Au(1)	144.38(2)
Au(1)#1-Tl(1)-Au(1)	146.72(2)
N(3)-Tl(2)-N(4)	61.9(3)
N(3)-Tl(2)-S(4)	109.2(2)
N(4)-Tl(2)-S(4)	67.4(2)
N(3)-Tl(2)-Au(2)	98.5(2)
N(4)-Tl(2)-Au(2)	118.3(2)

S(4)-Tl(2)-Au(2)	66.37(6)
C(1)-Au(1)-C(7)	174.0(5)
C(1)-Au(1)-Tl(1)#2	87.4(4)
C(7)-Au(1)-Tl(1)#2	98.0(4)
C(1)-Au(1)-Tl(1)	87.9(4)
C(7)-Au(1)-Tl(1)	86.3(4)
Tl(1)#2-Au(1)-Tl(1)	138.13(2)
C(13)-Au(2)-C(19)	172.8(6)
C(13)-Au(2)-Tl(1)	90.6(4)
C(19)-Au(2)-Tl(1)	94.7(4)
C(13)-Au(2)-Tl(2)	87.6(4)
C(19)-Au(2)-Tl(2)	94.9(4)
Tl(1)-Au(2)-Tl(2)	113.08(2)
Au(3)-Tl(3)-Au(4)#3	148.79(2)
Au(3)-Tl(3)-Au(4)	68.732(18)
Au(4)#3-Tl(3)-Au(4)	141.06(2)
N(1)-Tl(4)-N(2)	64.0(4)
N(1)-Tl(4)-Au(3)	98.5(3)
N(2)-Tl(4)-Au(3)	122.0(2)
C(25)-Au(3)-C(31)	172.6(6)
C(25)-Au(3)-Tl(3)	90.7(4)
C(31)-Au(3)-Tl(3)	96.4(4)
C(25)-Au(3)-Tl(4)	84.4(4)
C(31)-Au(3)-Tl(4)	95.6(4)
Tl(3)-Au(3)-Tl(4)	107.42(2)
C(43)-Au(4)-C(37)	177.0(6)
C(43)-Au(4)-Tl(3)#4	89.8(4)
C(37)-Au(4)-Tl(3)#4	89.0(4)
C(43)-Au(4)-Tl(3)	90.0(4)
C(37)-Au(4)-Tl(3)	92.5(4)
Tl(3)#4-Au(4)-Tl(3)	145.40(2)

[a] Symmetry transformations used to generate equivalent atoms: #1 -x,y+1/2,-z+1/2; #2 -x,y-1/2,-z+1/2; #3 -x+1,y-1/2,-z+1/2; #4 -x+1,y+1/2,-z+1/2.

Table S5. Population analysis (%) for model systems **2a**.

Model	Orbitals	Au	Tl	L_2	C_6F_5
2a	LUNO+4	8	44	30	18
	LUMO+3	18	76	5	1
	LUMO+2	18	50	20	13
	LUMO+1	12	13	74	1
	LUMO	5	8	86	1
	HOMO	29	38	28	5
	HOMO-1	24	1	1	74
	HOMO-2	13	2	5	81
	HOMO-3	2	1	3	95
	HOMO-4	15	3	5	77
	HOMO-5	31	9	49	11
	HOMO-6	1	1	92	6
	HOMO-7	12	3	84	1
	HOMO-8	22	9	47	23
	HOMO-9	19	2	19	59
	HOMO-10	11	3	85	2

Table S6. Population analysis (%) for model systems **3a**.

Model		L_1	Au	Tl	C_6F_5
3a	LUMO+5	17	19	47	17
	LUMO+4	86	3	8	3
	LUMO+3	0	17	74	9
	LUMO+2	7	28	48	17
	LUMO+1	92	3	4	2
	LUMO	68	23	8	1
	HOMO	49	16	29	6
	HOMO-1	3	17	3	77
	HOMO-2	0	5	1	93
	HOMO-3	96	1	3	0
	HOMO-4	2	20	3	75

Table S7. Population analysis (%) for model systems **4a**.

Model	Orbitals	Au	Tl	L_2	C_6F_5
16a	LUMO+4	22	45	17	16
	LUMO+3	22	46	21	10
	LUMO+2	17	20	61	1
	LUMO+1	27	43	7	23
	LUMO	7	13	79	1
	HOMO	21	4	0	75
	HOMO-1	61	16	9	14
	HOMO-2	4	6	0	89
	HOMO-3	3	1	1	95
	HOMO-4	17	5	4	74
	HOMO-5	24	17	4	55
	HOMO-6	24	34	22	20
	HOMO-7	8	8	15	69
	HOMO-8	7	2	9	83
	HOMO-9	20	22	43	15
	HOMO-10	9	11	38	42
	HOMO-11	12	3	27	59
	HOMO-12	12	6	10	72
	HOMO-13	14	7	77	2
	HOMO-14	11	2	84	2

Table S8. TD-DFT first Singlet-Singlet Excitation Calculations and Lowest Singlet-Triplet Excitations for Model system **2a**.

Model	exc.	λ_{calc} (nm)	ƒ (s)	contributions
2a	$S_0 \rightarrow S_7$:	290.1	0.0323	HOMO-6 → LUMO (92)
	$S_0 \rightarrow S_9$:	281.8	0.1417	HOMO → LUMO+2 (84)
	$S_0 \rightarrow S_{10}$:	271.8	0.0240	HOMO-10 → LUMO (38)
				HOMO-8 → LUMO (19)
				HOMO-6 → LUMO+1 (22)
	$S_0 \rightarrow S_{11}$:	268.5	0.0100	HOMO-7 → LUMO (78)
	$S_0 \rightarrow S_{12}$:	264.8	0.0866	HOMO → LUMO+4 (81)
	$S_0 \rightarrow S_{13}$:	261.5	0.0258	HOMO → L UMO+3 (83)
	$S_0 \rightarrow S_{15}$:	257.4	0.0105	HOMO-1 → LUMO+1 (73)
	$S_0 \rightarrow S_{18}$:	252.6	0.1026	HOMO-1 → LUMO+2 (82)
	$S_0 \rightarrow T_1$:	497.6	0.0000	HOMO-6 → LUMO (74)

Table S9. TD-DFT first Singlet-Singlet Excitation Calculations and Lowest Singlet-Triplet Excitations for Model system **3a**.

Model	exc.	λ_{calc} (nm)	ƒ (s)	contributions
3a	$S_0 \rightarrow S_1$:	401.9	0.0105	HOMO→LUMO (47.5)
	$S_0 \rightarrow S_9$:	332.9	0.1130	HOMO(-1)→LUMO+2 (23.9)
				HOMO→LUMO+2 (22.2)
	$S_0 \rightarrow S_{10}$:	330.2	0.2016	HOMO(-1)→LUMO+2 (22.9)
				HOMO→LUMO+2 (23.4)
	$S_0 \rightarrow S_{14}$:	321.4	0.0192	HOMO(-1)→LUMO+3 (39.5)
	$S_0 \rightarrow S_{17}$:	317.4	0.0501	HOMO(-4)→LUMO+2 (40.8)
	$S_0 \rightarrow S_{20}$:	312.1	0.1018	HOMO(-1)→LUMO+5 (32.4)

Table S10. TD-DFT first Singlet-Singlet Excitation Calculations and Lowest Singlet-Triplet Excitations for Model system **4a**.

Model	exc.	λ_{calc} (nm)	ƒ (s)	contributions
4a	$S_0 \rightarrow S_5$:	321.4	0.0268	HOMO-7 -> LUMO (27)
				HOMO-4 → LUMO (41)
	$S_0 \rightarrow S_6$:	320.3	0.1385	HOMO-1 → LUMO+1 (51)
				HOMO → LUMO+1 (43)
	$S_0 \rightarrow S_7$:	319.7	0.0780	HOMO-1 → LUMO+1 (40)
				HOMO → LUMO+1 (54)
	$S_0 \rightarrow S_{15}$:	284.8	0.0168	HOMO-11 → LUMO (33)
				HOMO-10 → LUMO (55)
	$S_0 \rightarrow S_{16}$:	283.7	0.0768	HOMO-4 → LUMO+1 (86)
	$S_0 \rightarrow S_{17}$:	279.2	0.0657	HOMO-5 → LUMO+1 (78)
	$S_0 \rightarrow S_{18}$:	274.9	0.0261	HOMO-14 → LUMO (45)
	$S_0 \rightarrow S_{19}$:	272.2	0.0634	HOMO-1 → LUMO+2 (44)
				HOMO-1 → LUMO+4 (28)
	$S_0 \rightarrow S_{20}$:	271.1	0.0240	HOMO-1 → LUMO+4 (39)
	$S_0 \rightarrow T_1$:	492.44	0.0000	HOMO-11 → LUMO (17)
				HOMO-10 → LUMO (28)

Table S11. Details of data collection and refinement for complex **1·½**toluene**.**

Compound	**1·½**toluene
Empirical formula	$C_{40}H_{26}AuF_{10}N_4S_2Tl\cdot$ ½ C_7H_8
Formula weight	1263.67
Temperature/K	173(2)
Crystal system	Triclinic
Space group	P-1
a/Å	10.2443(2)
b/Å	12.5801(4)
c/Å	16.2644(6)
α/°	95.3490(10)
β/°	90.880(2)
γ/°	102.923(2)
Volume/Å^3	2032.66(11)
Z	2
ρ_{calc}g/cm^3	2.065
μ/mm^{-1}	7.751
F(000)	1201.0
Crystal size/mm^3	0.375 × 0.15 × 0.05
Radiation	MoK_α (λ = 0.71073 Å)
2Θ range for data collection/°	4.876 to 54.984º
Reflections collected	31281
Independent reflections	9163 [R_{int} = 0.0529]
Data/restraints/parameters	9163/18/560
Goodness-of-fit on F^2	1.016
Final R indexes [I>=2σ (I)]	R_1 = 0.0468, wR_2 = 0.1159
Final R indexes [all data]	R_1 = 0.0663, wR_2 = 0.1272
Largest diff. peak/hole / e Å^{-3}	2.55/-2.93

Table S12. Details of data collection and refinement for complex **2**.

Compound	**2**
Empirical formula	$C_{30}H_{24}AuF_{10}N_2OS_2Tl$
Formula weight	1083.97
Temperature/K	173(2)
Crystal system	Monoclinic
Space group	$P2_1/c$
a/Å	12.4601(7)
b/Å	14.1891(7)
c/Å	18.1610(5)
α/°	90
β/°	100.255(3)
γ/°	90
Volume/Å^3	3159.5(3)
Z	4
ρ_{calc}g/cm^3	2.279
μ/mm^{-1}	9.952
F(000)	2032.0
Crystal size/mm^3	0.3 × 0.1 × 0.1
Radiation	MoK_α (λ = 0.71073 Å)
2Θ range for data collection/°	4.558 to 54.946º
Reflections collected	36518
Independent reflections	7166 [R_{int} = 0.0877]
Data/restraints/parameters	7166/0/424
Goodness-of-fit on F^2	1.038
Final R indexes [I>=2σ (I)]	R_1 = 0.0515, wR_2 = 0.1185
Final R indexes [all data]	R_1 = 0.0729, wR_2 = 0.1289
Largest diff. peak/hole / e Å^{-3}	2.89/-2.06

Table S13. Details of data collection and refinement for complex **3**·¼CH_2Cl_2**.**

Compound	**3**·¼CH_2Cl_2
Empirical formula	$C_{52}H_{26}Au_2F_{20}N_4S_2Tl_2$·¼ CH_2Cl_2
Formula weight	1970.36
Temperature/K	173(2)
Crystal system	Monoclinic
Space group	$P2_1/n$
a/Å	14.6658(4)
b/Å	22.7807(6)
c/Å	17.0613(5)
α/°	90
β/°	111.4930(10)
γ/°	90
Volume/Å^3	5303.8(3)
Z	4
ρ_{calc}g/cm^3	2.468
μ/mm^{-1}	11.784
F(000)	3626.0
Crystal size/mm^3	0.2 × 0.15 × 0.075
Radiation	MoK_α (λ = 0.71073 Å)
2Θ range for data collection/°	4.402 to 54.966
Reflections collected	51381
Independent reflections	12090 [R_{int} = 0.0833]
Data/restraints/parameters	12090/518/662
Goodness-of-fit on F^2	1.047
Final R indexes [I>=2σ (I)]	R_1 = 0.0639, wR_2 = 0.1573
Final R indexes [all data]	R_1 = 0.1065, wR_2 = 0.1801
Largest diff. peak/hole / e Å^{-3}	3.07/-2.56

Table S14. Details of data collection and refinement for complex **4**·¼CH_2Cl_2**.**

Compound	**4**·¼CH_2Cl_2
Empirical formula	$C_{42}H_{24}Au_2F_{20}N_2OS_2Tl_2$·¼ CH_2Cl_2
Formula weight	3681.31
Temperature/K	103(2)
Crystal system	Monoclinic
Space group	$P2_1/c$
a/Å	30.557(4)
b/Å	11.0238(12)
c/Å	29.803(4)
α/°	90
β/°	109.107(4)
γ/°	90
Volume/Å^3	9486.2(19)
Z	8
ρ_{calc}g/cm^3	2.578
μ/mm^{-1}	13.173
F(000)	6724.0
Crystal size/mm^3	0.37 × 0.14 × 0.03
Radiation	MoK_α (λ = 0.71073 Å)
2Θ range for data collection/°	5.488 to 55.894
Reflections collected	205050
Independent reflections	22695 [R_{int} = 0.1117]
Data/restraints/parameters	22695/1419/1288
Goodness-of-fit on F^2	1.110
Final R indexes [I>=2σ (I)]	R_1 = 0.0673, wR_2 = 0.1279
Final R indexes [all data]	R_1 = 0.0979, wR_2 = 0.1394
Largest diff. peak/hole / e Å^{-3}	3.04/-3.04

Computational studies: DFT calculations and population analysis

In the case of the binuclear model **2a**, the population analysis (Table S5) of the highest occupied molecular orbital (HOMO) shows that it is mainly localized on the metal centers Au(I) and Tl(I) (67%) with a small contribution from the ligand $\mathbf{L_2}$ (28%), the lowest empty molecular orbital (LUMO) is mainly localized on the ligand unit (86%) (Figure S1). Furthermore, while occupied frontier molecular orbitals from HOMO-1 to HOMO-4 are mostly located on the C_6F_5- moieties with a small contribution of Au(I), those from HOMO-5 to HOMO-10 show a mixed Au(I)/C_6F_5-/$\mathbf{L_2}$ character with a higher contribution of the $\mathbf{L_2}$ fragment. Finally, with the exception of LUMO+1 where the electronic density is mainly localized on the ligand unit, the MOs from LUMO+2 to LUMO+4 show a mixed Au(I)/Tl(I) prevailing character (Figure S1).

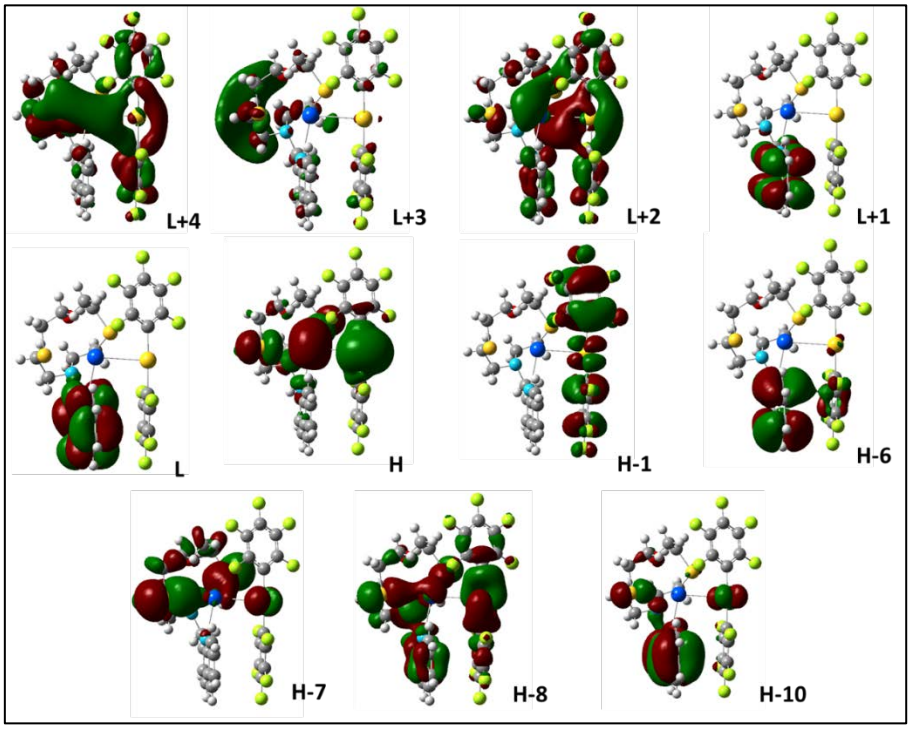

Figure S1. Most important frontier molecular orbitals (isovalue = 0.02) for model system **2a** (L=LUMO; H=HOMO).

A different behavior can be observed for the tetranuclear molecular model [{Au(C_6F_5)$_2$Tl}{Au(C_6F_5)$_2$}{Tl(**L_1**)}] **3a**. In fact, the population analysis (Table S6) of the HOMO shows that it is mainly located on the ligand **L_1** (49%) and the metal centers [Au(I)/Tl(I) 45%]; while, with the exception of HOMO-3 whose electronic density is mainly localized on the organic ligand **L_1** (93%), MOs from HOMO−1 to HOMO−4 are characterized by a significant contribution from the C_6F_5- moieties (75-93%) (Figure S2). On the other hand, the population analysis of the lowest empty orbital (LUMO) shows a main contribution from **L_1** (68%) with a small contribution from gold atoms (23%), while the LUMO+2, LUMO+3 and LUMO+5 orbitals are mainly located on the metallic fraction. Finally, the LUMO+1 and LUMO+4 are mainly located on the ligand **L_1** (Figure S2).

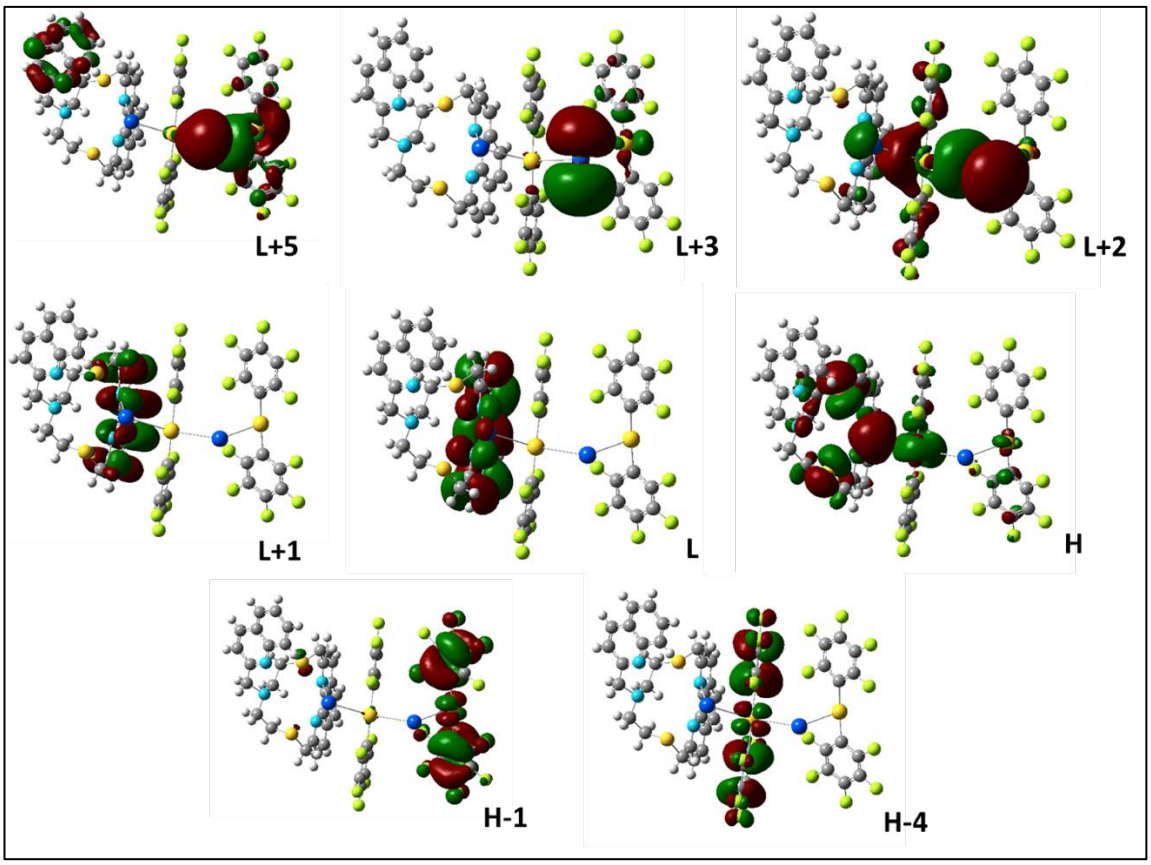

Figure S2. Most important frontier molecular orbitals (isovalue = 0.02) for model system **3a** (L=LUMO; H=HOMO).

Model **4a** shows common features with the previous models but also some differences. While the HOMO orbital is mainly located on the $[Au(C_6F_5)_2]^-$ moiety, the LUMO orbital, as in model **2a**, displays predominantly an $\mathbf{L_2}$ character with the electron density mainly localized on the quinoline fragment (Table S7, Figure S3). The rest of occupied molecular orbitals from HOMO-1 to HOMO-14 show in general a strong contribution of the $C_6F_5^-$ units with a smaller contribution from each metal; some exceptions are observed: HOMO-5 and HOMO-6 show a significant contribution from the metal centers; HOMO-13 and HOMO-14 are prevailingly located on the ligand $\mathbf{L_2}$ (Table S7, Figure S3). Finally, the rest of empty molecular orbitals from LUMO+1 to LUMO+4 show a strong contribution of Au(I)/Tl(I) metals with the only exception of LUMO+2 that present a greater contribution of $\mathbf{L_2}$ with the electronic density again mainly localized on the quinoline moiety (Table S7, Figure S3).

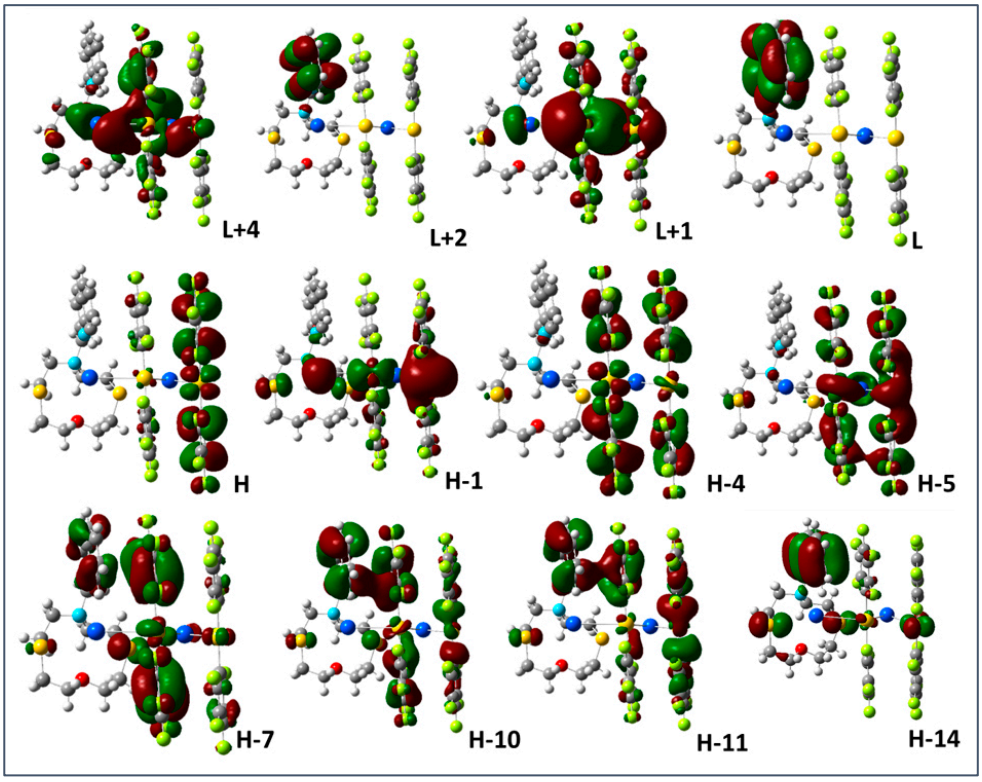

Figure S3. Most important frontier molecular orbitals (isovalue = 0.02) for model system **4a** (L = LUMO; H = HOMO).